Characterization of dynamic speckle sequences using principal component analysis and image descriptors

José M. López-Alonso [a], Eduardo Grumel [b], Nelly L. Cap [b], Marcelo Trivi [b], Héctor Rabal [b] and Javier Alda [a]

[a]Applied Optics Complutense Group, University Complutense of Madrid, Ave. Arcos de Jalón, 118. 28037 Madrid. Spain

[b] Centro de Investigaciones Ópticas (CONICET La PlataCIC), Facultad de Ingenieríia, Universidad Nacional de La Plata, Casilla de Correo 3, 1897 Gonnet- La Plata, Argentina

ABSTRACT

Speckle is being used as a characterization tool for the analysis of the dynamic of slow varying phenomena occurring in biological and industrial samples. The retrieved data takes the form of a sequence of speckle images. The analysis of these images should reveal the inner dynamic of the biological or physical process taking place in the sample. Very recently, it has been shown that principal component analysis is able to split the original data set in a collection of classes. These classes can be related with the dynamic of the observed phenomena. At the same time, statistical descriptors of biospeckle images have been used to retrieve information on the characteristics of the sample. These statistical descriptors can be calculated in almost real time and provide a fast monitoring of the sample. On the other hand, principal component analysis requires longer computation time but the results contain more information related with spatial-temporal pattern that can be identified with physical process. This contribution merges both descriptions and uses principal component analysis as a pre-processing tool to obtain a collection of filtered images where a simpler statistical descriptor can be calculated. The method has been applied to slow-varying biological and industrial processes

Keywords: Principal components analysis, dynamic speckle, LASCA, Fujii, Generalized Differences

1. INTRODUCTION

Speckle analysis and speckle interferometry have been used to obtain deformations, topography, roughness characteristics, and also, when considered dynamically, to know the temporal evaluation of changes in the shape of observed objects.[1] Several speckle analysis techniques have used the variations in intensity, and polarization, to obtain the desired parameters. Most of the analysis techniques are heuristic in origin, and their objective is mainly practical and adapted for a given environment or application. Artificial intelligence techniques have been incorporated, along with learning algorithms (supervised and non supervised), and the segmentation and identification of regions of interest within data.[2,3] However, there is not an unique strategy for analyzing dynamic speckle images applicable to a wide variety of situations.

In this contribution we compare the outcomes of two well established methods: Principal Component Analysis (PCA), and image descriptors. PCA is a multivariate technique that has been successfully applied to characterize several kinds of spatial temporal phenomena.[4] Noise and digital compression algorithms have been evaluated using PCA. Its statistical foundations make this approach safe and sound, providing spatial and temporal information of interest for the given case.[5,6] On the other hand, statistical descriptors, have been proposed and used to resume in a single number or as a map the overall characteristics of the phenomena.[7,8] These descriptors are usually simpler than the results from PCA and are computationally more economic from the point of view of time of calculation and resources allocation. On the other hand, PCA requires an additional layer of knowledge to be included within the analysis. As any other computational method, PCA always produces a result. These

Further author information: (Send correspondence to Javier Alda)
Javier Alda: E-mail: javier.alda@ucm.es, Telephone: +34.91.3946874

Optics and Photonics for Information Processing IX, edited by Abdul A. S. Awwal, Khan M. Iftekharuddin, Mohammad A. Matin, Mireya García Vázquez, Andrés Márquez, Proc. of SPIE Vol. 9598, 95980Q

results need expert interpretation for the given case. This makes PCA more user dependent, specially when reaching meaningful conclusions.

The application of PCA to biospeckle images has been already considered with quite promising results.[8,9] The approach used in this paper is to apply PCA to a given sequence of dynamic speckle images. PCA produces several results that can interpreted as filtered or rectified sequences. Then, the overall descriptors will be applied to the original and PCA-filtered sequences to infer more information and see how these methods may work together to provide better insight of the phenomena under analysis. The input data used in this paper consist of two video sequences of dynamic speckle. One of the sequences corresponds with the drying evolution of a coin, and the other is obtained by registering the speckle images of a bruised apple.

Section 2 explains how PCA works for a temporally ordered collection of speckle frames (a dynamic speckle sequence). At the same time we briefly present the results obtained from PCA and how they can explain the inner dynamics of the data. Then, in section 3 we define the overall descriptors that are calculated for each case obtained before. Finally, section 4 summarizes the main conclusions obtained in this contribution.

2. PRINCIPAL COMPONENT ANALYSIS

PCA has been widely used in a variety of fields and situations. Its main ability is to reduce the dimension of data collections, and to extract the most meaningful components and structures. In this contribution we focus our attention to the character of the data. They are collections of frames taken at a given temporal rate. They can be seen as a video sequence. At the same time, as far as they are obtained by coherent illumination they show a speckle pattern that changes along time due to variations in the observed specimen. In a very first approach, PCA can be seen as a rotation transformation from a $N-$dimensional coordinate system to a new $N-$dimensional coordinate system where the frames show no correlation.

The results of PCA for a video sequence having N frames, F_i, and M pixels, has the following three main results:

- Eigenvalues, λ_i, where i runs from 1 to N. These eigenvalues represent the variance given by each one of the principal components. From these values it is possible to calculate the relative weight, w_i, of each principal component dividing its value by the sum of the N eigenvalues: $w_i = \lambda_i / \sum_{i=1}^{N} \lambda_i$.
- Principal components, PC_i $(i = 1 \dots N)$. They are the new "frames" that show no correlation.
- Eigenvectors, E_i. These eigenvectors can be arranged as a $N \times N$ unitary matrix that describes the rotation between the actual frames, F_i, and the Principal Components, PC_i.

Some subtle considerations need to be given here in order to understand better the results extracted from PCA. First of all, the original frames have to be converted in a new collection of frames having zero mean. This means that it is necessary to subtract the mean of each frame to each one. These zero-mean frames are the ones transformed by the PCA rotation. This is important when retrieving a filtered sequence. On the other hand, principal components, although showing no correlation, could be connected by inner data uncertainties. This fact allows a grouping of principal components into processes.[5] In those cases where the eigenvalues are isolated, the associated eigenvalues show a temporal behavior close to a harmonic variation.[10] Then, it is possible to relate each isolated eigenvalue to a given temporal frequency. Using these concepts it is possible to classify the set of N principal components in several subsets showing different correlation properties. This will be explained more in detail in subsection 2.1. As a consequence of this classification strategy it is possible to reconstruct a filtered version of the original sequence taking into account a selected collection of principal components. This has been done and makes possible a clear interpretation of the results. At the same time, it produces new sets of frames that can be analyzed with global descriptors.

Using the previous assumptions and properties of PCA we have applied it to three collections of frames taken at a frame rate of 1.25 fps.

- Collection A: Video sequence of the drying process of a coin. 398 frames, each frame having 512×512 pixels.

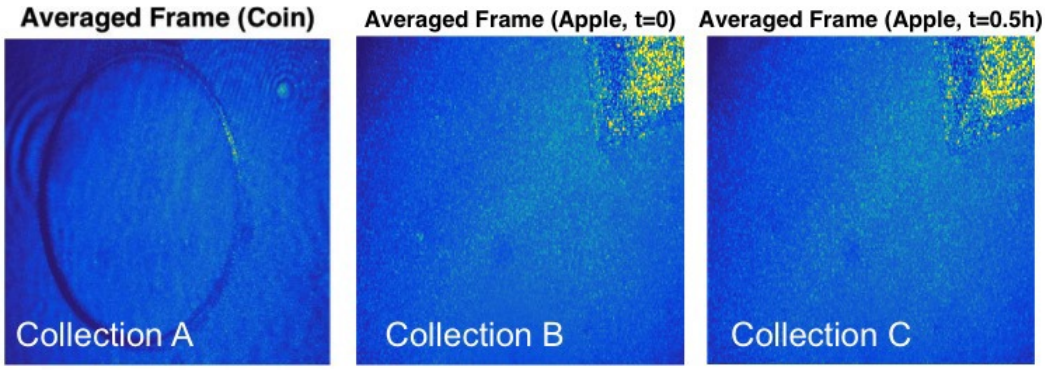

Figure 1. Mean of the frames for each data collection. Collection A is for the coin and collections B and C are for the apple.

Table 1. Classification of the principal components into classes

	P1 (A ; B; C)	P2 (A ; B; C)	P3 (A ; B ; C)
# range	[1:30] ; [1:36] ; [1:34]	[31:68] ; [37:127] ; [35:113]	[69:398] ; [128:500] ; [114:500]
Relative weight: $\sum_{i\in P} w_i$	0.8717 ; 0.7692 ; 0.7803	0.0749 ; 0.0945 ; 0.0818	0.0534 ; 0.1363 ; 0.1379

- Collection B: Video sequence of an apple mechanically beaten and taken just after the beat. 500 frames, each frame having a 300×300 pixelss.
- Collection C: Video sequence of an apple mechanically beaten and taken after 30 minutes since the beat. 500 frames, each frame having a 300×300 pixels.

Figure 1 shows the average frame for each collection. The shape of the coin is clearly seen in collection A, The triangular shape in the right top corner of the image is a reference non-biological object. The apple is beaten at the center of the bottom region of the image.

2.1 Results from the PCA

As we previously mentioned, we have focused our attention in the classification of the obtained principal components. First of all we have analyzed both the eigenvalues and the temporal spectrum of the eigenvectors. In the first row of Fig. 2 we have plotted the eigenvalues for each set of frames in semilog graph. The vertical lines limit three different classes classified using the PCA results.

This classification works as follows. The first class, P1, comprises all the principal components, eigenvalues and eigenvectors, characterized by an isolated eigenvalue. Isolation is defined after checking the uncertainties in the eigenvalue coming from the statistics of the data collection (see Appendix in ref[5]). The third class, P3, represents all the components that are represented by eigenvalues that can be grouped together in a single process. This means that the uncertainties in these eigenvalues overlap successively. Finally, the second class, P2, is defined using the intermediate principal components between classes P1 and P3. Table 1 summarizes the results obtained from this classification. At the same, we have calculated that the first principal component, PC#1, accounts for 0.4153, 0.5372, and 0.5616 of the total variance for the coin and the two apple sequences respectively.

As a matter of fact, the harmonic character of the eigenvectors is much clearer for the first eigenvectors (see middle row in Fig. 2) than for the eigenvectors corresponding to principal components of higher rank number.

Besides these preliminary results obtained from PCA, after classifying the components into classes, we may reconstruct the original data taking into account only those principal components included in each class (see # range in Table 1). In figure 3 we present the original object before painting, and one of the frames for the original sequences, and the three sequences filtered using the previously defined classes. We may notice in images d) and e) of Fig. 3 the profile of the coin can be slightly perceived as local diminished contrast. Filtered sequences can

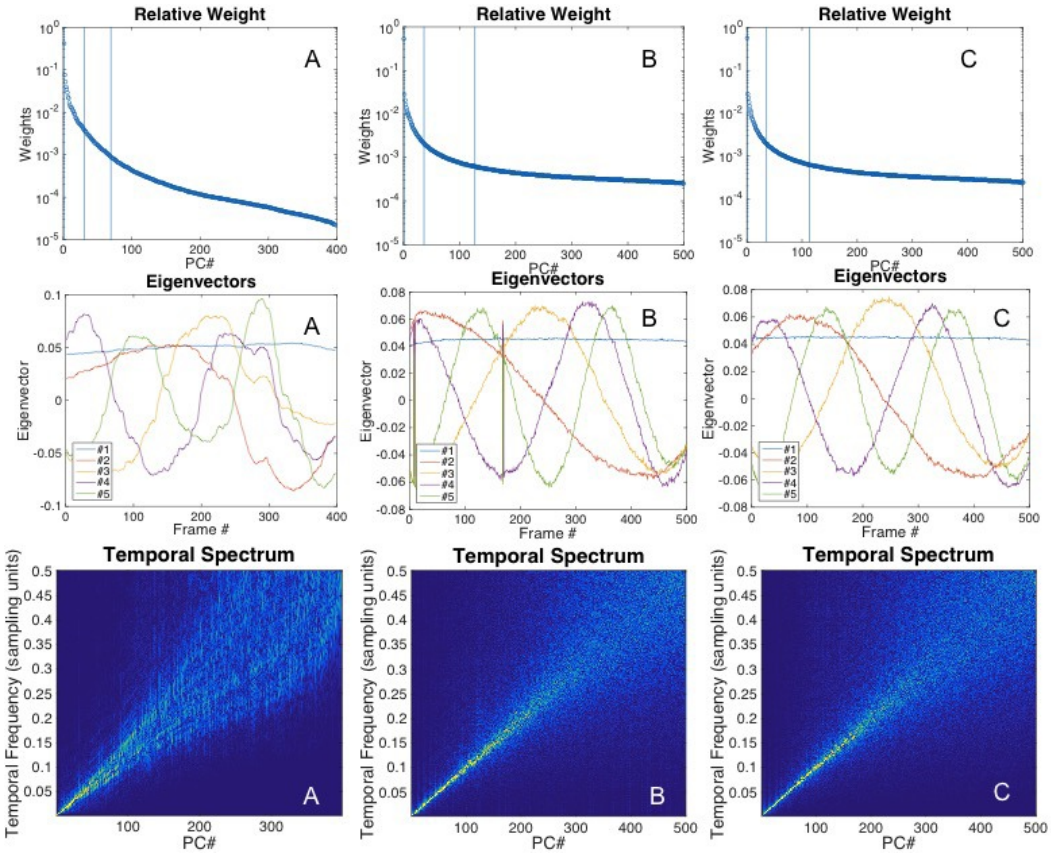

Figure 2. The columns correspond with the coin (A) and apple (B and C) sequences respectively. The relative weights, w_i, are plotted in the first row. The vertical lines denote the separation between different classes of dynamics classified in this paper. The first five eigenvectors are plotted in the central row. We may see how the dependence is quite close to a harmonic variation. Finally, the spectrum of the eigenvectors is plotted as a map for both set of sequences at the third row.

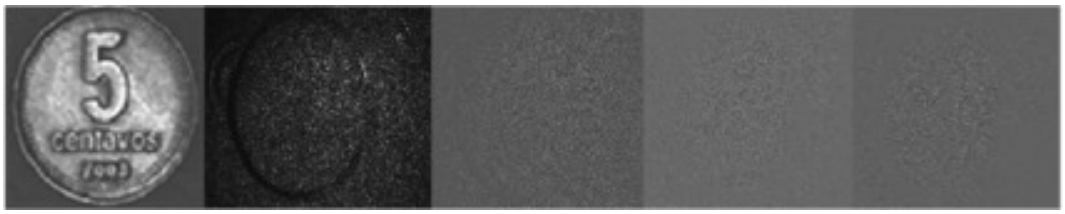

Figure 3. The original object is represented when illuminated by incoherent light a), and coherent light b). Images c), d) and e) are frames extracted from the three filtered sequences P1, P2, and P3 respectively.

be treated statistically and some results are easily found. Some preliminary results have been obtained when evaluating the map standard deviation of the frames for the third class. The map of this figure of merit has been included in Fig. 4. From these figures we can see how the hidden topography is revealed. This parameter will be also considered as a descriptor in the next section.

3. MAP'S DESCRIPTORS

Some global and local descriptors have been proposed to determine the spatial and temporal characteristics of a dynamic speckle analysis. Some of the findings of the analysis shown in this paper are related with the spatial identification of temporal phenomena. Then, it seems reasonable to focus our attention in time-domain

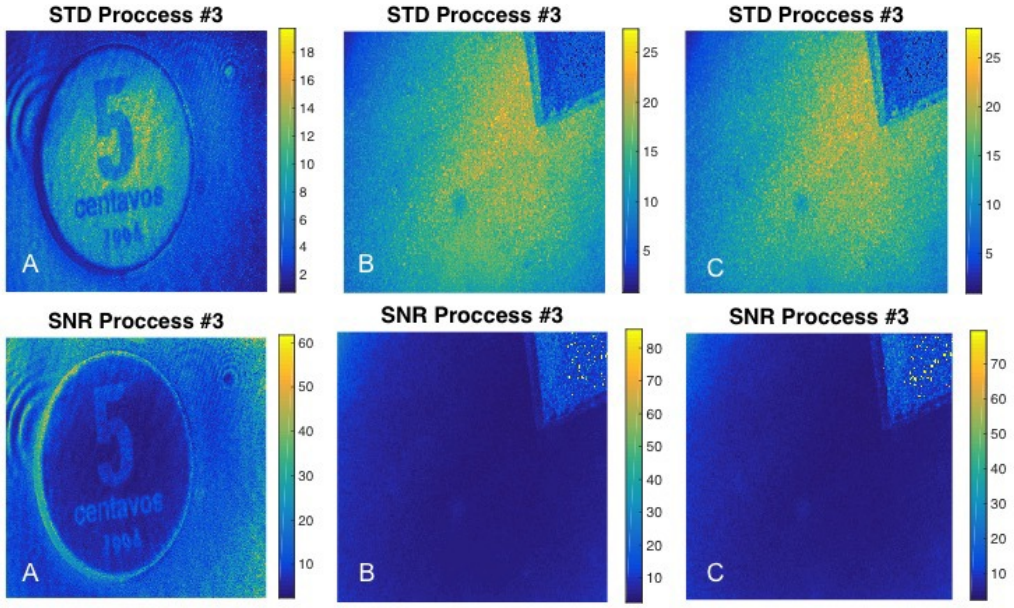

Figure 4. The columns correspond with the coin (A) and apple (B and C) sequences respectively. The maps on top of this figure represent the standard deviation for each pixel of the frames calculated along the whole sequence (398 frames for the coin and 500 frames for the apple). The maps at the bottom are for the signal-to-noise ratio calculated as the ratio between the mean and standard deviation for each pixel in the image along the whole sequences.

descriptors. They are given in terms of the value of the pixel located at a position (i, j), at a given frame, k, of the full N frames sequence: $x_k(i, j)$. Because of its importance in the medical applications, we also include one more (LASCA) that requires only one frame for its calculation. These descriptors will be easily represented as maps. They are listed as follows.

- **Standard Deviation (STD):** This parameter is calculated as the standard deviation along the frames for each pixel. Figure 4 presents the map of this value of the third class of processes defined from the PCA results. In this figure we also map the signal-to-noise ratio (SNR) defined as the quotiente between the mean and the standard deviation along the time for each pixel. STD It is given by:

$$\mathrm{STD}(i,j) = \sigma = \sqrt{\frac{1}{N}\sum_{k=1}^{N}\left(x_k(i,j) - \mu(i,j)\right)^2}, \tag{1}$$

  where $\mu(i,j) = \frac{1}{N}\sum_{k=1}^{N} x_k(i,j)$, is the mean value of the pixel (i, j) along the sequence.

- **Generalized Differences (GD):** It takes into account the intensity variation at various time scales.[11] It is given by:

$$\mathrm{GD}(i,j) = \frac{1}{N}\sum_{k=1}^{N}\sum_{l=1}^{N-k}\left|x_k(i,j) - x_{k+l}\right|. \tag{2}$$

- **Weighted Generalized Differences (WGD):** A variation of the GD parameter is defined by weighting the importance of consecutive frames in the sequence. This is made by defining a weight that works as a temporal window. This weight is denoted as p, and takes a non-zero value only in those frames around the given frame. By doing this, the variation is enhanced when appearing temporarily close to the frame. It is defined as:

$$\mathrm{WGD}(i,j) = \sum_{k=1}^{N}\sum_{l=1}^{N-k}\left|x_k(i,j) - x_{k+l}\right| p(l). \tag{3}$$

A typical form of $p(l)$ is a collection of 1 for several frames (5, 7, ...) around the central frame (k), being the rest of the values of $p(l) = 0$.

- **Substraction average of consecutive differences (AVD):** It is defined as the addition of consecutive differences along the sequence.[12] It is defined as:

$$\mathrm{AVD}(i,j) = \frac{1}{N-1}\sum_{k=1}^{N-1} \left| x_k(i,j) - x_{k+1} \right|. \tag{4}$$

- **Fujii's Differences (Fujii):** This parameter is also a variation of the AVD parameter.[13] It can be seen as the mean value of the temporal contrast between consecutive frames:

$$\mathrm{Fujii}(i,j) = \frac{1}{N-1}\sum_{k=1}^{N-1} \left| \frac{x(i,j)_k - x(i,j)_{k+1}}{x(i,j)_k + x(i,j)_{k+1}} \right| \tag{5}$$

- **Laser Contrast Analysis (LASCA):** This parameter takes into account the ratio of spatial standard deviation to the mean value on a predefined spatial window around each pixel. When the sample is active within the given spatial window, the signals are averaged and the contrast is lower. Then, active regions produce low values of this parameter.

These parameters have been calculated for the collection of frames obtained from the PCA. In figure 5 we show the results of evaluating the descriptors at P1, P2 and P3 classes in the coin experiment. For comparison, in the first column we include the result obtained when the algorithms are applied to the unfiltered frames. The same pseudocoloring palette was used in all of them to decrease subjective biases. The maps are normalized to the maximum value for each one. The first column shows unfiltered GD results. The details of the coin cannot be perceived for the original frames. The same happens in class P1, which is very similar. P2 shows some details and P3 permits clear recognition of the number "5, the word "centavos" and the year "1994. In the second row we show the corresponding results of the application of WGD. The unfiltered result shows under-surface details that can be recognized. P1 shows scarce details covered with a speckle pattern. P2 and P3 show progressively higher quality. The following row shows LASCA results. For the current integration time of the camera in the registered speckle patterns, no detail can be perceived. P1 also shows no details. P2 shows very noisy details, and P3 shows perceivable number, letters and noisy date. As the processing involves a 3×3 pixels squared moving spatial window, all results show some tiling and reduced resolution. Then, in the next row, we can see the calculation of the standard deviation, STD. This parameter has been already presented in figure 4 for class P3 in the coin and apple data sets. Here, STD does not show a good performance for the original and P1 sequences. P2 shows some details, and P3 shows the topographic details. The fifth row shows the maps of the AVD descriptor. Here, the image obtained with unfiltered AVD is already very informative. In the filtered ones, quality improves as we move from P1 to P3. Class P3 results compares very well with the results obtained from original unfiltered frames. This result is the best obtained with filtered images The Fujii descriptor is given in the last row. For the application of Fujii algorithm, the results are excellent for the original data. Class P1 is almost not informative at all and dark, class P2 is better and class P3 is the best of this series. Topographic details can be readily perceived and read.

The bruised apple sequences have been treated in the same way as the coin. However, in this case, we are more interested in retrieving some information about the bio-activity of the sample. This is why we have performed the analysis to two sets of frames taken at different times: one sequence (collection B) is taken immediately after the apple has been bruised, and the second sequence is taken after half an hour (collection C). The results of STD and Fujii descriptors are given in figure 6 for the original and the three filtered sequences. In some of these images a faint dark small region can be hardly perceived in the center of the bruised region. This result agrees with former assessments of the bruising described in the literature.

When considering the maps of the STD parameter we can see that the unfiltered result does not show a perceivable image of the change in activity due to the bruising. In class P1 the bruised region is clearly perceived

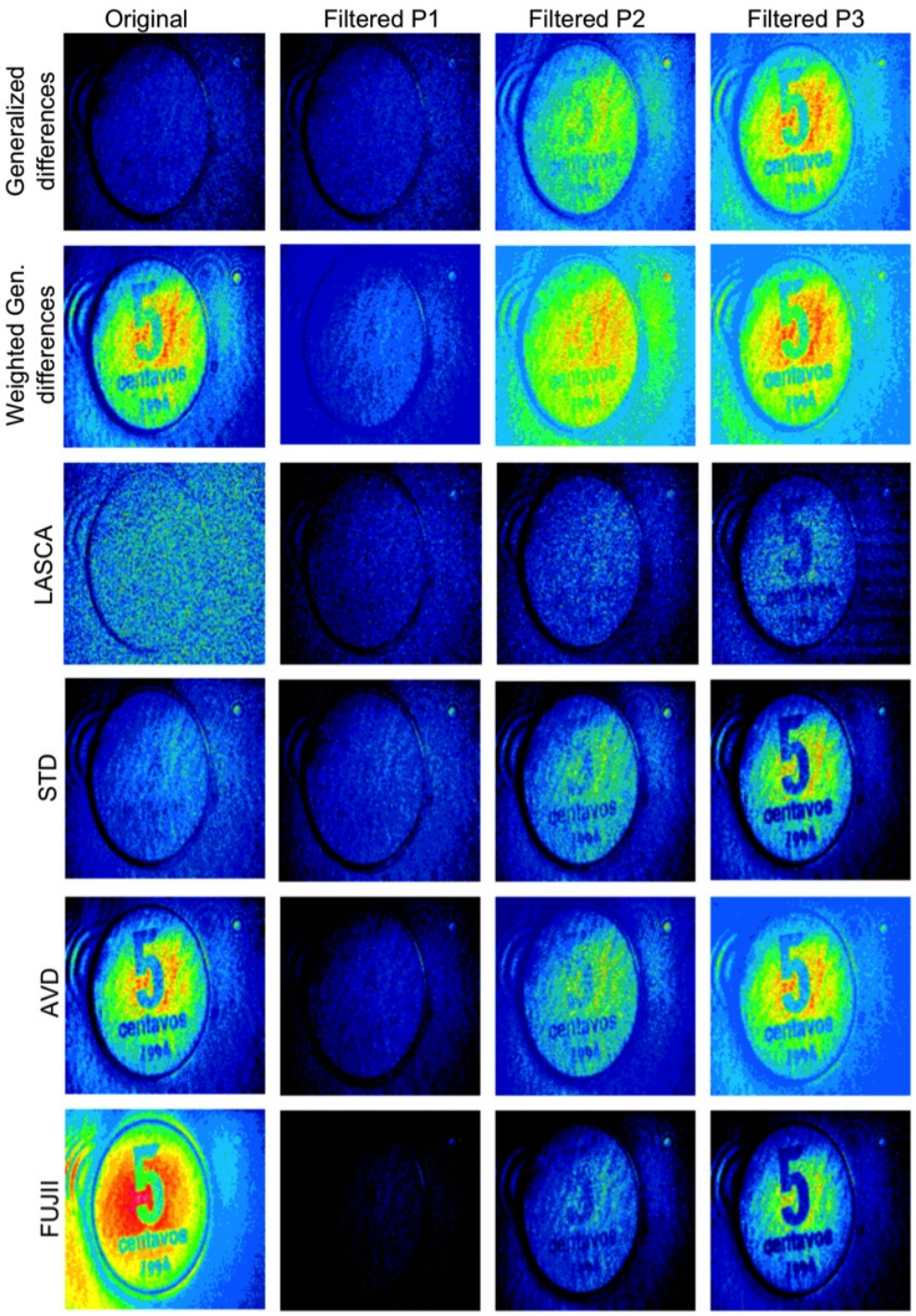

Figure 5. Maps for the descriptor applied to the original and filtered sequences for the coin data.

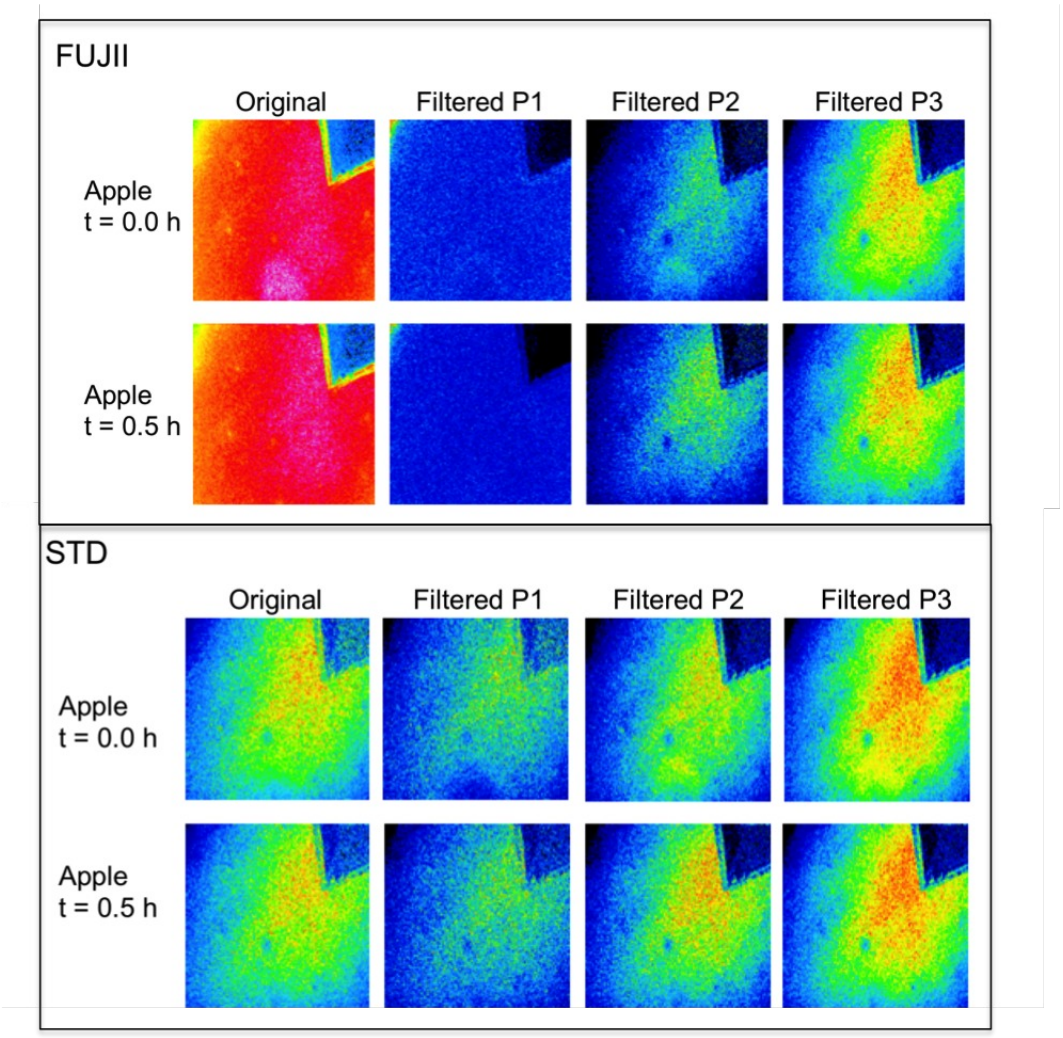

Figure 6. Maps of the STD and Fujii descriptors applied to the original and filtered sequences for two apple's sequences.

as a semicircular dark region in the lower side. Class P2 shows this part as a croissant like bright region and Class P3 does not clearly distinguish the bruised region from the healthy rest. Fujii algorithm is here tested for time 0 (immediately after the hit) and $t = 0.5$ h. The first image shows the unfiltered result. The bruised region is clearly apparent. Then class P1 image is mostly uninformative, P2 shows a faint croissant like bright region surrounding the bruised region, and again P3 does not clearly distinguish the bruised form the remaining healthy regions of the apple.

4. CONCLUSIONS

The application of the PCA to biospeckle images makes possible a spatial-temporal description of the data. PCA slices the variance of the data into uncorrelated images. In the literature, PCA is usually used to compress images, among other applications, and the principal aim is to reduce the dimensionality and to keep only the most energetic components where the interesting information is assumed to be present. In this contribution we exemplify the analysis by two study cases that appear in the literature: that of the topography under drying paint on a coin, and the bruising of an apple that cannot be perceived before processing. After applying PCA, the most contributing images are associated with harmonic temporal variations. Besides, these principal components are independent and cannot be connected through the noise of the data. On the other hand, those principal

components with the lowest contributions can be grouped together because of the inner statistics relations among data. This grouping strategy defines three classes of sequences: the first one represents most of the variance of the original data and it is linked with a power spectrum density. The third class represents noise variations beyond the Nyquist frequency related with the acquisition rate. In between these two classes there is another one that defines intermediate time scales.

For the coin drying data, the analysis of the original data produces topographic results for the WGD, AVD, and Fujii parameters. However, this analysis cannot be associated with the quantitative evaluation of the involved time scales. This can be done using the results of PCA, where the three filtered sequences are associated to three different time scales. In the coin case, the application of the descriptors shows that the topography under paint is mostly contained in class P3, corresponding to low eigenvalues. It is evident that the principal components required for the description of the speckle images bear most energy in the speckles themselves while the interesting information for our experiment is mostly contained in the smaller ones. For the bruised apple experiment the result shows that this is not always the case. When calculating the STD descriptor for filtered images in class P1 the place of the bruising is easily perceived as a dark region. It is detected then because there is less energy there than in the healthy rest of the apple. In several of the filtered and processed images the results are good and eventually better than in the unfiltered ones. So, that even if nicer results for viewing are shown by Fujii algorithm in both experiments, PCA decomposition informs in which time-scale band is present the phenomenon (topography or bruised region) that the experiment intends to explain. Through the use of PCA, time scales can be assigned to the PCA class so that a link to present physical phenomena could be guessed.

Summarizing these results we may see that PCA is capable of revealing hidden contributions to the speckle variations. These contributions are related to separable time scales. This fact makes possible a quantitative and qualitative spatial-temporal description of the phenomena under analysis. Besides, the application of speckle descriptors to the filtered sets of data improves the capability of identification of underlying biological or time-dependent processes. Further improvement can be expected if diferent descriptors are combined by using supervised or no supervised neural networks.

ACKNOWLEDGMENTS

This work has been supported by the Ministerio de Economia y Competitividad of Spain through the project TEC2013-40442, and CONICET, CIC and UNLP, Argentina.

REFERENCES

[1] Rabal, H. and Braga, R. A., [*Dynamic Laser Speckle and Applications*], CRC Press (2008).

[2] Passoni, I., Rabal, H., Meschino, G., and Trivi, M., "Probabitlity mapping images in dynamic speckle classification," *Appl. Opt.* **52**, 726–733 (2013).

[3] Passoni, L. I., Dai Pra, A. L., Scandura, A., Meschino, G., Weber, C., Guzman, M., Rabal, H. J., Trivi, M., and Estevez, P. A., "Improvement in the visualization of segmente areas of patterns of dynamic speckle classification," in [*Advances in Self-Organizing Maps*], **198**, 163–171, AISC (2013).

[4] Jolliffe, I. T., [*Principal component analysis*], Springer Series in Statistics, Springer, Berlin (2002).

[5] Lopez-Alonso, J. M., Alda, J., and Bernabeu, E., "Principal components characterization of noise for infrared images," *Appl. Opt.* **41**, 320–331 (2002).

[6] Lopez-Alonso, J. M. and Alda, J., "Characterization of artifacts in fully digital image-acquisition systems: Application to web cameras," *Opt. Eng.* **43**(1), 257–265 (2004).

[7] Sendra, G. H., Dai Pra, A. L., Passoni, L. I., Arizaga, R., Rabal, H. J., and Trivi, M., "Biospeckle descriptors: a performance comparison," *Proc. SPIE* **7387**, 73871K–73871K–5 (2010).

[8] Nassif, R., Nader, C. A., Afif, C., Pellen, F., Le Brun, G., Le Jeune, B., and Abboud, M., "Detection of golden's apple climacteric peak by laser biospeckle mesasurements," *Appl. Opt.* **53**(35), 8276–8262 (2014).

[9] Lopez-Alonso, J. M., Alda, J., Rabal, H. J., Grumel, E., and Trivi, M., "Dynamic speckle analysis using multivariate techniques," *J. Opt.* **17**(3), 035609 (2015).

[10] Lopez-Alonso, J. M. and Alda, J., "Operational parameterization of the 1/f noise of a sequence of frames by means of the principal component analysis in focal plane arrays," *Opt. Eng.* **42**, 1915–1922 (2003).

[11] Arizaga, R., Cap, N., Rabal, H. J., and Trivi, M., "Display of local activity using dynamical speckle patterns," *Opt. Eng.* **41**(2), 287–294 (2002).

[12] Braga, J. R., Silva, B., Rabelo, G., Marques, R., Enes, A., Cap, N., Rabal, H. J., Arizaga, R., Trivi, M., and Horgan, G., "Reliability of biospeckle image analysis," *Opt. Lasers Eng.* **45**(3), 390–395 (2007).

[13] Fujii, H., Nohira, K., Yamamoto, Y., Ikawa, H., and Ohura, T., "Evaluation of blood flow by lsaer speckle image sensing. part i," *Appl. Opt.* **24**(24), 5321–5325 (1987).